# Weakly nonlinear analysis of boundary layer receptivity to free-stream disturbances

L. Brandt and D. S. Henningson[a)]
*Department of Mechanics, KTH, S-10044 Stockholm, Sweden*

D. Ponziani
*Department of Mechanics and Aeronautics, University of Rome "La Sapienza," 18 Via Eudossiana, 00184 Rome, Italy*

(Received 12 March 2001; accepted 10 January 2002; published 5 March 2002)

The intent of the present paper is to study the receptivity of a zero pressure gradient boundary layer to free-stream disturbances with the aim to isolate the essential features involved in the generation of streamwise streaks. A weakly nonlinear formulation based on a perturbation expansion in the amplitude of the disturbance truncated at second order is used. It is shown that the perturbation model provide an efficient tool able to disentangle the sequence of events in the receptivity process. Two types of solutions are investigated: the first case amounts to the receptivity to oblique waves generated by a wave-like external forcing term oscillating in the free stream, the second the receptivity to free-stream turbulence-like disturbances, represented as a superposition of modes of the continuous spectrum of the Orr–Sommerfeld and Squire operators. A scaling property of the governing equations with the Reynolds number is also shown to be valid. The relation between this nonlinear receptivity process and previously investigated linear ones is also discussed. © *2002 American Institute of Physics.* [DOI: 10.1063/1.1456062]

## I. INTRODUCTION

The objective of the present work is the study of the stability and receptivity of the boundary layer subjected to free-stream disturbances. From a theoretical point of view, boundary layer stability has traditionally been analyzed in terms of the eigensolutions of the Orr–Sommerfeld, Squire equations that reduces the study to exponentially growing disturbances. Experimental findings show that transition due to turbulence in the free stream is mainly characterized by the occurrence of streamwise elongated structures which are very different from the exponentially growing perturbations. These streamwise structures (or streaks) were first identified by Klebanoff[1] in terms of low frequency oscillations in hot wire signals caused by low spanwise oscillations of the streaks (Kendall,[2] Westin *et al.*[3]) and are commonly referred to as Klebanoff modes.

Further analysis of the Orr–Sommerfeld, Squire equations (Gustavsson,[4] Butler and Farell,[5] Reddy and Henningson,[6] and Trefethen *et al.*[7]) have confirmed that disturbances other than exponentially growing perturbations may lead to disturbance growth. From a mathematical point of view this is due to the non-normality of the Orr–Sommerfeld, Squire operator. The physical mechanism behind this linear mechanism is the lift-up induced by streamwise vortices that interact with the boundary layer shear thus generating streaks in the streamwise velocity component. Transition due to these types of disturbances is generally called bypass transition.

The understanding and prediction of transition require the knowledge of how a disturbance can enter and interact with the boundary layer, commonly referred to as receptivity of the boundary layer. The disturbances are often characterized as either acoustic or vortical disturbances convected by the free stream. Both types of disturbances have been investigated by asymptotic methods and a summary of the results can be found in the reviews by Goldstein and Hultgren[8] and Kerschen.[9] Bertolotti[10] has assumed as initial disturbances vortical modes, solutions of the linearized Navier–Stokes equations in the free steam, which are waves periodic in the spanwise direction and decaying in the streamwise and has studied the boundary layer receptivity in a ''linear region'' excluding the leading edge. He has found receptivity to modes with zero streamwise wave number and has shown that the growth is most likely connected to the theories of nonmodal growth. To answer the question of which disturbance present at the leading edge gives the largest disturbance in the boundary layer at a certain downstream position, Andersson, Berggren, and Henningson,[11] and Luchini[12] have used an optimization technique adapted from optimal-control theory. The disturbances they found were also streamwise vortices that caused the growth of streaks, and both the wall normal disturbance shape and growth rates agreed well with the findings of Bertolotti[10] and to experimental results. Wundrow and Goldstein[13] used asymptotic expansions to study the effects of a small amplitude steady streamwise vorticity field on the flow over a flat plate. Their results show how an initially linear perturbation of the upstream flow leads to strong nonlinear shear layers far downstream of the leading edge.

Berlin and Henningson[14] have carried out numerical ex-

a)Author to whom correspondence should be addressed. Electronic mail: henning@mech.kth.se

 

periments on how simple vortical free-stream disturbances interact with a laminar boundary layer, and have identified a linear and a new nonlinear receptivity mechanism. The nonlinear one was found to force streaks inside the boundary layer similar to those found in experiments on free-stream turbulence and it worked equally well for streamwise and oblique free-stream disturbances. The boundary layer response caused by the nonlinear mechanism was, depending on the initial disturbance energy, comparable to that of the linear mechanism, which was only efficient for streamwise disturbances.

In the present work we develop a theoretical analysis with the aim to isolate the features involved in the generation of streamwise streaks in flows subjected to free-stream turbulence. We consider a weakly nonlinear model based on a perturbation expansion in terms of the amplitude of the disturbance, truncated at second order. The model, originally developed in a previous work for Poiseuille flow (Ponziani[15] and Ponziani *et al.*[16]), is here extended to boundary layer flows. This implies the inclusion of the continuous spectrum eigenfunctions in the representation of the first and the second order solutions. To validate the model we first investigate a receptivity mechanisms in a boundary layer imposing a localized disturbance both in the boundary layer and in the free stream. In particular, we study the long time response of the system to a couple of oblique modes oscillating with a given frequency $\omega$. For this case the linearized stability equations are driven at first order by the external disturbance and at second order by the quadratic interactions between first order terms. For the type of disturbance considered, the presence of oblique waves generates streamwise vortices which, in turn, induce the formation of streaks inside the boundary layer. The oblique modes are associated to $(\alpha, \pm\beta)$ wave numbers and their quadratic interactions produce $(0, 2\beta)$ wave numbers that correspond, in physical terms, to an elongated vortical structure, i.e., streamwise counter-rotating vortices. The results show that the generation of streamwise vorticity, which is a nonlinear mechanism, and its subsequent lift-up can indeed be recovered through the weakly nonlinear formulation. The theory is validated through comparison of the results obtained in this case with direct numerical simulations.

The model is then applied to investigate the response of the boundary layer to continuous spectrum modes. The latter are fundamental for the understanding of the interaction between free-stream vortical eddies and the boundary layer since they reduce to simple sines and cosines in the free stream and can easily be used to represent a free-stream turbulence spectrum. By using continuous modes, which are solutions of the linear problem, the model reduces to solve a second order equation where the forcing is given by the weakly nonlinear interactions between continuous modes. An extensive parametric study is carried out to analyze the interaction between Orr–Sommerfeld as well as Squire modes, in particular considering the effect of the disturbance wave numbers. A scaling property of the resolvent of the Orr–Sommerfeld and Squire problem with the Reynolds number is shown to be valid for the results obtained.

## II. THE PERTURBATION MODEL

In the following we define the streamwise, wall normal and spanwise directions as $x$, $y$, and $z$, respectively, with velocity perturbation $\underline{u}=(u,v,w)$. All variables are made dimensionless with respect to the constant displacement thickness $\delta_0^*$ and the free-stream velocity $U_\infty$ (time is made nondimensional with respect to $\delta_0^*/U_\infty$). The perturbation equations are derived directly from the Navier–Stokes equations where we have superimposed a perturbation field to the base flow, namely the Blasius profile. We consider no-slip boundary conditions at the wall, solenoidal initial conditions and in order to impose periodic boundary conditions in the directions parallel to the wall we assume a parallel base flow. Although the parallel flow assumption is questionable in the limit of low streamwise wave numbers $(\alpha\to 0)$, its use is supported by the works of Berlin and Henningson[14] and Tumin and Reshokto,[17] among others. They show in fact, that the generation of streamwise streaks is due to the same physical mechanism and that the transient growth of streamwise independent optimal disturbances is similar for the parallel and nonparallel case.

We study the evolution of a disturbance in a boundary layer over a flat plate via perturbation theory by expanding the relevant variables in terms of the amplitude of the disturbance $\epsilon$

$$\begin{aligned} \underline{u} &= \underline{u}^{(0)} + \epsilon\underline{u}^{(1)} + \epsilon^2\underline{u}^{(2)} + \cdots, \\ p &= p^{(0)} + \epsilon p^{(1)} + \epsilon^2 p^{(2)} + \cdots, \end{aligned} \tag{1}$$

where $\underline{u}^{(0)}, p^{(0)}$ is the given base flow, while remaining terms are unknowns to be determined by the perturbation analysis. We consider a general case in which the perturbation equations are forced by an external forcing

$$F(x,y,z,t) = \epsilon F^{(1)}(x,y,z,t),$$

with a given initial condition.

Substituting the expansion (1), truncated at second order, into the Navier–Stokes equations and collecting terms of like powers in $\epsilon$, one obtains the governing equations for the first and the second order. These equations can be rewritten in the normal velocity $v^{(j)}$, normal vorticity $\eta^{(j)}(j=1,2)$ formulation, thus obtaining the following Orr–Sommerfeld, Squire system

$$\left[\left(\frac{\partial}{\partial t} + u^{(0)}\frac{\partial}{\partial x}\right)\Delta - D^2u^{(0)}\frac{\partial}{\partial x} - \frac{1}{\mathrm{Re}}\Delta^2\right]v^{(j)} = N_v^{(j)} + F_v^{(j)}, \tag{2}$$

$$\left[\frac{\partial}{\partial t} + u^{(0)}\frac{\partial}{\partial x} - \frac{1}{\mathrm{Re}}\Delta\right]\eta^{(j)} + Du^{(0)}\frac{\partial v^{(j)}}{\partial z} = N_\eta^{(j)} + F_\eta^{(j)}, \tag{3}$$

where

$$N_v^{(j)} = -\left[\left(\frac{\partial^2}{\partial x^2} + \frac{\partial^2}{\partial z^2}\right)S_2^{(j)} - \frac{\partial^2}{\partial x\partial y}S_1^{(j)} - \frac{\partial^2}{\partial y\partial z}S_3^{(j)}\right], \tag{4}$$

$$N_\eta^{(j)} = -\left(\frac{\partial}{\partial z}S_1^{(j)} - \frac{\partial}{\partial x}S_3^{(j)}\right) \tag{5}$$

with

$$S_1^{(j)}=\frac{\partial}{\partial x}u^{(j-1)}u^{(j-1)}+\frac{\partial}{\partial y}u^{(j-1)}v^{(j-1)}+\frac{\partial}{\partial z}u^{(j-1)}w^{(j-1)}, \tag{6}$$

$$S_2^{(j)}=\frac{\partial}{\partial x}u^{(j-1)}v^{(j-1)}+\frac{\partial}{\partial y}v^{(j-1)}v^{(j-1)}+\frac{\partial}{\partial z}v^{(j-1)}w^{(j-1)}, \tag{7}$$

$$S_3^{(j)}=\frac{\partial}{\partial x}u^{(j-1)}w^{(j-1)}+\frac{\partial}{\partial y}v^{(j-1)}w^{(j-1)}+\frac{\partial}{\partial z}w^{(j-1)}w^{(j-1)}. \tag{8}$$

The first and second order equations have constant coefficients with respect to the streamwise and spanwise directions, hence we consider the Fourier transform in the $(x,z)$ plane by making the following form assumption for the solution $q^{(j)}=(v^{(j)},\eta^{(j)})^T$:

$$q^{(j)}(x,y,z,t)=\sum_m\sum_n \hat{q}_{mn}^{(j)}(y,t)e^{i(\alpha_m x+\beta_n z)}$$

and likewise for the external forcing. The wave numbers are defined as follows:

$$\alpha_m=m2\pi/L_x, \tag{9}$$

$$\beta_n=n2\pi/L_z, \tag{10}$$

$$k_{mn}^2=\alpha_m^2+\beta_n^2, \tag{11}$$

where $L_x$ and $L_z$ are, respectively, the streamwise and spanwise lengths of the periodic domain. Hereafter, for reading convenience, the subscript $m$ and $n$ are omitted and we refer to the equations for the individual wave number $(\alpha_m,\beta_n)$ as $(\alpha,\beta)$. The resulting equations in matrix form read

$$\left(\frac{\partial}{\partial t}\hat{M}-\hat{L}\right)\hat{q}^{(1)}=\hat{P}\hat{F}, \tag{12}$$

$$\left(\frac{\partial}{\partial t}\hat{M}-\hat{L}\right)\hat{q}^{(2)}=\hat{P}\sum_{k+p=m}\sum_{l+q=n}[\hat{N}(\underline{\hat{u}}_{kl}^{(1)}\underline{\hat{u}}_{pq}^{(1)^T})]^T, \tag{13}$$

where

$$\hat{L}=\begin{pmatrix}\mathcal{L}_{\mathrm{OS}} & 0\\ \mathcal{C} & \mathcal{L}_{\mathrm{SQ}}\end{pmatrix},\quad \hat{M}=\begin{pmatrix}k^2-D^2 & 0\\ 0 & 1\end{pmatrix},$$

$$\hat{N}=\begin{pmatrix}i\alpha\\ D\\ i\beta\end{pmatrix},\quad \hat{P}=\begin{pmatrix}-i\alpha D & k^2 & -i\beta D\\ -i\beta & 0 & i\alpha\end{pmatrix}.$$

$\hat{L}$ is the linear operator that defines the classical Orr–Sommerfeld, Squire problem

$$\mathcal{L}_{\mathrm{OS}}=i\alpha u^{(0)}(D^2-k^2)-i\alpha D^2u^{(0)}-\frac{1}{\mathrm{Re}}(D^2-k^2)^2,$$

$$\mathcal{C}=-i\beta Du^{(0)}, \tag{14}$$

$$\mathcal{L}_{\mathrm{SQ}}=-i\alpha u^{(0)}+\frac{1}{\mathrm{Re}}(D^2-k^2).$$

We introduce the inner product and the corresponding energy norm associated to the kinetic energy of the disturbance velocity according to

$$E=\int_0^\infty \hat{q}^H\hat{M}\hat{q}\,dy=(\hat{M}\hat{q},\hat{q})=\|\hat{q}\|_E. \tag{15}$$

In this investigation we consider two different types of solutions. In the first case the system of equations at first order is forced by an external force that we assume pulsating with a given frequency $\omega$,

$$\hat{F}^{(1)}=\hat{f}(y)e^{i\omega t}+\hat{f}^*(y)e^{-i\omega t},$$

where the $*$ indicates the complex conjugate. At second order, the problem is forced by the nonlinear interactions of first order terms

$$\hat{T}=\hat{P}\sum_{k+p=m}\sum_{l+q=n}[N(\underline{\hat{u}}_{kl}^{(1)}\underline{\hat{u}}_{pq}^{(1)^T})]^T. \tag{16}$$

In the second case, we assume that the solution for the first order is given by a continuous spectrum mode representation, and we solve only the second order problem.

The initial conditions are

$$\hat{q}^{(j)}(t=0)=\hat{q}_0,\quad j=1,2. \tag{17}$$

With regard to the boundary conditions we enforce no-slip conditions

$$\hat{v}^{(j)}=D\hat{v}^{(j)}=\hat{\eta}^{(j)}=0 \tag{18}$$

while we assume boundedness in the free stream. The remaining velocities are recovered by

$$\hat{u}^{(j)}=\frac{i}{k^2}(\alpha D\hat{v}^{(j)}-\beta\hat{\eta}^{(j)}), \tag{19}$$

$$\hat{w}^{(j)}=\frac{i}{k^2}(\beta D\hat{v}^{(j)}+\alpha\hat{\eta}^{(j)}). \tag{20}$$

### A. The solution to the forced problem

We consider here the harmonically forced problem described by the system of Eqs. (12) and (13) whose solution can be split into two parts (see Ponziani *et al.*[16]): one representing the long time asymptotic solution $\hat{q}^{(j)^L}$ and the other describing the initial transient behavior $\hat{q}^{(j)^T}$,

$$\hat{q}^{(j)}=\hat{q}^{(j)^T}+\hat{q}^{(j)^L},\quad j=1,2. \tag{21}$$

First we consider the equations for the long time behavior at first order

$$
\begin{aligned}
&(\pm i\omega\hat{M}-\hat{L})\hat{q}^{(1)^L}=\hat{P}\hat{F},\\
&\hat{v}^{(1)^L}=D\hat{v}^{(1)^L}=\hat{\eta}^{(1)^L}=0, \quad y=0, \quad y=y_\infty
\end{aligned}
\tag{22}
$$

whose long time response to the harmonic forcing is given by

$$
\hat{q}^{(1)^L}_{\pm\omega}=(\pm i\omega\hat{M}-\hat{L})^{-1}\hat{P}\hat{f}(y)e^{\pm i\omega t}. \tag{23}
$$

The equations that describe the transient at first order are given by

$$
\begin{aligned}
&\frac{\partial}{\partial t}\hat{M}\hat{q}^{(1)^T}=\hat{L}\hat{q}^{(1)^T},\\
&\hat{q}^{(1)^T}=-\hat{q}^{(1)^L}, \quad t=0,\\
&\hat{v}^{(1)^T}=D\hat{v}^{(1)^T}=\eta^{(1)^T}=0, \quad y=0, \quad y=y_\infty,
\end{aligned}
\tag{24}
$$

where we have assumed zero initial conditions, $\hat{q}_0=0$. Equations (22) and (24) provide a complete description of the harmonic forced linear problem; the solution of Eq. (24) is obtained as described in a later section.

With regard to the second order solution, the structure of the quadratic interaction term implies that several frequency components are excited at second order. As for the first order problem we can split the governing equations into two parts that describe the long time and the transient behavior. With regard to the former, we point out that at first order the asymptotic solution in time is characterized by given frequencies $\pm\omega$, which implies that only the zero and $2\omega$ frequency components are excited at second order. However, as demonstrated by Trefethen *et al.*,[7] the maximum response of a system occurs for $\alpha=0$ and $\omega=0$; hence we reduce our analysis to the most effective part, that is the one associated to zero frequency and zero streamwise wave number

$$
-\hat{L}\hat{q}_0^{(2)^L}=\hat{T}_0^L \tag{25}
$$

with solution given by

$$
\hat{q}_0^{(2)^L}=(-\hat{L})^{-1}\hat{T}_0^L. \tag{26}
$$

Here the terms $\hat{T}_0^L$ represent the convolution sum in (16) where only the contribution with zero frequency is considered. Observe that this procedure can also be applied to the solution corresponding to the continuous spectrum modes. Indeed, if a first order solution is represented as a continuous spectrum mode, it is still characterized by a given frequency that corresponds to the real part of the associated eigenvalue.

The equations that describe the transient behavior at second order accounts for different forcing terms that arise from the self-interactions between first order transient solutions and the quadratic interactions between the transient solution and the long time solutions.

### B. Scaling of forced solution

It is possible to show a Reynolds number dependence for the norm of the resolvent of the forced problems defined by Eqs. (23) and (26). Let us introduce a new set of variables to rescale the Orr–Sommerfeld, Squire problem as Gustavsson,[4] Reddy and Henningson,[6] and Kreiss *et al.*,[18]

$$
t^*=t/\mathrm{Re}, \quad i\omega^*=i\omega\,\mathrm{Re}, \quad \hat{v}^*=\hat{v}/\beta\,\mathrm{Re}, \quad \hat{\eta}^*=\hat{\eta}; \tag{27}
$$

with the new scaling we can rewrite (14) as

$$
\begin{aligned}
&\mathcal{L}^*_{\mathrm{OS}}=i\alpha\,\mathrm{Re}\,u^{(0)}(D^2-k^2)-i\alpha\,\mathrm{Re}\,D^2u^{(0)}-(D^2-k^2)^2,\\
&\mathcal{C}^*=-iDu^{(0)},\\
&\mathcal{L}^*_{\mathrm{SQ}}=-i\alpha\,\mathrm{Re}\,u^{(0)}+(D^2-k^2).
\end{aligned}
\tag{28}
$$

The scaled equations exhibit a dependency only on the two parameters, $\alpha\,\mathrm{Re}$ and $k^2$, rather than $\alpha,\beta,\mathrm{Re}$ as in the original Orr–Sommerfeld, Squire equations. In the new variables the resolvent can be written as

$$
\|(i\omega\hat{M}-\hat{L})^{-1}\|_E=\mathrm{Re}\|(i\omega^*\hat{M}-\hat{L}^*)^{-1}\|_{E^*}, \tag{29}
$$

where $E$ is the energy norm with respect to the original variables and $E^*$ is the energy norm with respect to the scaled ones. It is possible to show, see Kreiss *et al.*,[18] that for $\alpha\,\mathrm{Re}=0$ (that corresponds to the maximum response of the system) the norm of the resolvent $\|(i\omega^*\hat{M}-\hat{L}^*)^{-1}\|_{E^*}$ scales as the Reynolds number as $\mathrm{Re}\to\infty$. Hence, Eq. (29) implies that the norm of the original resolvent $\|(i\omega\hat{M}-\hat{L})^{-1}\|_E$ scales as the square of the Reynolds number.

Further, it is possible to show (see, e.g., Ref. 18) that if we consider Reynolds number independent forcing the amplitude of the response in the original unscaled problem is given at leading order, $O(\mathrm{Re}^2)$, by the wall normal vorticity $\eta$. In fact, for streamwise independent modes the norm of the resolvent of the individual Orr–Sommerfeld and Squire operators is $O(\mathrm{Re})$. The factor $\mathrm{Re}^2$ is then due to the response of the Squire operator forced by the $O(\mathrm{Re})$ wall normal velocity $v$, via the coupling term of the system. This implies that the induced streamwise vorticity, given by the solution of the Orr–Sommerfeld equation, is $O(\mathrm{Re})$, while the streamwise velocity, obtained from the Squire equation, is $O(\mathrm{Re}^2)$.

### C. The initial value problem

In accounting for the transient solution it is worth making some observations. Since the eigenfunctions of the eigenvalue problem associated to the Orr–Sommerfeld, Squire system form a complete set, see DiPrima and Habetler[19] and Salwen and Grosch,[20] we can expand the perturbation solution $\hat{q}^{(i)^T}$ $(i=1,2)$ as a superposition of modes. For Blasius boundary layer flow, the domain is semibounded and the spectrum has a continuous and a discrete part, see Grosch and Salwen.[21] These authors have shown that in this case the solution can be expanded in a sum over the discrete modes and in an integration over the continuous spectrum. This analysis can be simplified using a discrete representation of the continuous spectrum by cutting the upper unbounded domain at a given $y_\infty$. Although the eigenvalues differ from the exact representation of the continuous spectrum, particularly as the decay rate increases (see Fig. 2), their sum has been found to describe correctly the solution to the initial value problem, see Butler and Farrel.[5] Observe that formally, it is possible to expand the solution using integrals over the con-

tinuous spectrum. However, the added computational complexity, without any significant gain in accuracy, justifies the use of the present simpler formulation.

With regard to the selection of a set of functions that are orthogonal to the set of Orr–Sommerfeld, Squire eigenfunctions, we exploit the orthogonality relation between the eigenfunctions of the Orr–Sommerfeld, Squire system $(\tilde{q})$ and those of the adjoint Orr–Sommerfeld, Squire problem $(\tilde{q}^+)$. From the definition of adjoint, it is easy to show that the eigenvalues of the adjoint are the complex conjugate to the eigenvalue of the Orr–Sommerfeld, Squire system. This leads to the orthogonality condition

$$(\hat{M}\tilde{q}_j, \tilde{q}_k^+) = C\,\delta_{jk}, \tag{30}$$

where $\delta_{jk}$ is the Kronecker symbol and $C$ a constant that normalizes the eigenfunctions and that needs to be determined. Hence, for the initial value problem, we can exploit the completeness of the Orr–Sommerfeld, Squire eigenmodes for bounded flows to recover $\hat{q}^{(i)^T}$,

$$\begin{pmatrix} \hat{v}^{(i)^T} \\ \hat{\eta}^{(i)^T} \end{pmatrix} = \sum_l K_l \begin{pmatrix} \tilde{v}_l \\ \tilde{\eta}_l^P \end{pmatrix} e^{-i\lambda_l^{\mathrm{OS}} t} + \sum_j B_j \begin{pmatrix} 0 \\ \tilde{\eta}_j \end{pmatrix} e^{-i\lambda_j^{\mathrm{Sq}} t}, \tag{31}$$

where $(\lambda_l^{\mathrm{OS}}, \tilde{v}_l)$ and $(\lambda_j^{\mathrm{Sq}}, \tilde{\eta}_j)$, respectively, are the eigenvalues and eigenvectors of the non-normal $\mathcal{L}_{\mathrm{OS}}$ operator, and the homogeneous $\mathcal{L}_{\mathrm{SQ}}$ operator and $\tilde{\eta}_l^P$ is the solution of the Squire problem forced by the Orr–Sommerfeld eigenfunctions. The coefficient $K_l$ and $B_j$ are determined from a given initial condition $(\hat{v}_0, \hat{\eta}_0)$ according to (30),

$$K_l = \frac{1}{2k^2} \int_0^{y_\infty} \begin{pmatrix} \tilde{\xi}_l \\ 0 \end{pmatrix}^H \begin{pmatrix} k^2 - D^2 & 0 \\ 0 & 1 \end{pmatrix} \begin{pmatrix} \hat{v}_0 \\ \hat{\eta}_0 \end{pmatrix} dy, \tag{32}$$

$$B_j = \frac{1}{2k^2} \int_0^{y_\infty} \begin{pmatrix} \tilde{\xi}_j^P \\ \tilde{\zeta}_j \end{pmatrix}^H \begin{pmatrix} k^2 - D^2 & 0 \\ 0 & 1 \end{pmatrix} \begin{pmatrix} \hat{v}_0 \\ \hat{\eta}_0 \end{pmatrix} dy, \tag{33}$$

where

$$\begin{pmatrix} \tilde{\xi} \\ 0 \end{pmatrix}, \quad \begin{pmatrix} \tilde{\xi}^P \\ \tilde{\zeta} \end{pmatrix} \tag{34}$$

are the modes of the adjoint system, see Schmid and Henningson.[22]

### D. Continuous spectrum modes

The Orr–Sommerfeld eigenvalue problem in a semi-bounded domain is characterized by a continuous and a discrete spectrum. The discrete modes decay exponentially with the distance from the wall, while the modes of the continuous spectrum are nearly sinusoidal, whereby the free-stream disturbances can be expanded as a superposition of continuous modes. Since they are associated to stable eigenvalues, they are not relevant for the classical linear stability analysis; however they are fundamental for the understanding of the interaction between free-stream vortical eddies and the boundary layer. In order to determine the eigenfunctions of the continuous spectrum we consider first the Orr–Sommerfeld equations for a small three-dimensional (3D) disturbance with no-slip boundary conditions at the wall $\tilde{v}(0) = D\tilde{v}(0) = 0$ and boundedness at $y \to \infty$. In particular in the free stream the mean flow is constant (i.e., $u^{(0)} = 1$ as $y/\delta^* > 3$) and the Orr–Sommerfeld equation reduces to

$$(D^2 - k^2)^2 \tilde{v} - i\alpha\,\mathrm{Re}\{(1-c)(D^2 - k^2)\}\tilde{v} = 0, \tag{35}$$

where $c$ is the phase velocity. The above equation admits the following solution, see Grosch and Salwen:[21]

$$\tilde{v} = Ae^{i\gamma y} + Be^{-i\gamma y} + Ce^{-ky}, \quad y \to \infty, \tag{36}$$

where

$$k^2 + \gamma^2 + i\alpha\,\mathrm{Re}(1-c) = 0.$$

From this, an analytical expression for the eigenvalues is derived

$$c = 1 - i\left(1 + \frac{\gamma^2}{k^2}\right)\frac{k^2}{\alpha\,\mathrm{Re}}, \tag{37}$$

where $\gamma$ represents the wave number in the wall-normal direction and assumes any positive real value.

From a numerical point of view the crucial point is to enforce the boundedness of the eigenfunctions at $y \to \infty$. We follow the method introduced by Jacobs and Durbin[23] to recover the correct behavior of the solution in the free stream solving the equation as a two-point boundary value problem using the spectral collocation method based on Chebyshev polynomial.

We need a total of four boundary conditions: the first two are the no slip at the wall. The arbitrary normalization is $\tilde{v}(y_\infty) = 1$, where $y_\infty$ is the maximum value of $y$ in the wall-normal direction. The condition of boundedness as $y \to \infty$ is converted to a numerical condition at two specific values of $y$. In fact Eq. (36) implies

$$D^2\tilde{v} + \gamma^2\tilde{v} = C(k^2 + \gamma^2)e^{-ky} \tag{38}$$

in the free stream. The missing boundary condition is derived evaluating relation (38) at two different points in the free stream $y_1, y_2$,

$$\frac{(D^2\tilde{v} + \gamma^2\tilde{v})_{y_1}}{(D^2\tilde{v} + \gamma^2\tilde{v})_{y_2}} = e^{k(y_2 - y_1)}. \tag{39}$$

A similar procedure is used to determine the continuous modes of the Squire equation. However in this case the free-stream behavior of the solution is given only by the two complex exponentials. Hence, from a numerical point of view it suffices to enforce the arbitrary normalization condition $\tilde{\eta}(y_\infty) = 1$.

### E. The numerical method

The temporal eigenvalue systems and the forced problems derived in the preceding sections are solved numeri-

cally using a spectral collocation method based on Chebyshev polynomials. In particular, we consider the truncated Chebyshev expansion

$$\phi(\eta)=\sum_{n=0}^{N}\overline{\phi^n}T_n(\eta),$$

where

$$T_n(\eta)=\cos(n\arccos(\eta)) \tag{40}$$

is the Chebyshev polynomial of degree $n$ defined in the interval $-1\leqslant\eta\leqslant 1$, and the discretization points are the Gauss–Lobatto collocation points,

$$\eta_j=\cos\frac{\pi j}{N},\quad j=0,1,\ldots,N,$$

that is, the extrema of the $N$th-order Chebyshev polynomial $T_N$ plus the endpoints of the interval. The calculations are performed using at least 301 Chebyshev collocation points in $y$. The wall-normal domain varies in the range $(0,y_\infty)$, with $y_\infty$ well outside the boundary layer (typically $y_\infty=50$). The Chebyshev interval $-1\leqslant\eta\leqslant 1$ is transformed into the computational domain $0\leqslant y\leqslant y_\infty$ by the use of the mapping

$$y=y_\infty\frac{1-\eta}{2}. \tag{41}$$

The unknown functions $\hat{q}=\hat{q}(y)$ are then approximated by

$$\hat{q}^N(y)=\sum_{n=0}^{N}\overline{q^n}T_n(\eta).$$

The Chebyshev coefficients $\overline{q^n}$, $n=0,\ \ldots,N$ are determined by requiring the different equations derived from (12) and (13) to hold for $\hat{q}^N$ at the collocation points $y_j$, $j=p,\ \ldots,\ N-p$, with $p=2$ for the fourth order Orr–Sommerfeld equation and $p=1$ for the second order Squire equation. The boundary conditions are enforced by adding the equations

$$\sum_{n=0}^{N}\overline{q^n}T_n(0)=\sum_{n=0}^{N}\overline{q^n}T_n(y_\infty)=0,$$

and the two additional conditions for the Orr–Sommerfeld problem

$$\sum_{n=0}^{N}\overline{q^n}DT_n(0)=\sum_{n=0}^{N}\overline{q^n}DT_n(y_\infty)=0,$$

where $DT_n$ denotes the $y$ derivative of the $n$th Chebyshev polynomial.

## III. RECEPTIVITY TO LOCALIZED FORCING

### A. Disturbance generation and parameter settings

To validate the model, we test the analytical results versus direct numerical simulations of the type presented by Berlin and Henningson.[14] In order to trigger the formation of streamwise streaks in the boundary layer we consider the response of the system to a couple of oblique waves. This is similar to the investigations reported in Ref. 14, although here we are able to understand the mechanism in more detail since we use an analytical formulation. The oblique waves are generated by a harmonic localized wall-normal volume force given by

$$\underline{F}=f(y)\cos(\alpha x)\cos(\beta z)e^{i\omega t} \tag{42}$$

with

$$f(y)=\frac{1}{\sqrt{2\pi}\sigma}e^{-[(y-y_0)^2/2\sigma^2]}.$$

In our computations we choose Re=400, and $(\alpha,\pm\beta)=(0.2,\pm 0.2)$. We analyze two cases: for the first one the forcing is in the boundary layer ($y_0=2.2$), for the second the forcing is in the free stream ($y_0=8$). The results presented here correspond to the latter case with $\sigma=0.5$.

The formation of streamwise streaks in the boundary layer is initiated by two oblique waves characterized by wave numbers $(\alpha,\pm\beta)=(0.2,\pm 0.2)$. In the linear long time response of the system to the external forcing, there is no evidence of streaks generation. However, if one accounts for the second order interactions [in particular those that force the wave number $(0,\ 2\beta)$] it is easy to observe that the second order correction corresponds to a system of strong streamwise longitudinal vortices in the boundary layer. These results are in agreement with the work of Berlin and Henningson[14] where the generation of streaks in the boundary layer is triggered by the nonlinear evolution of two oblique waves.

### B. Comparison to DNS data: Linear and nonlinear case

In order to validate the perturbation model and its capability to select the most effective interactions as a second order correction, we compare our results with direct numerical simulations of the forced evolution problem and an initial value problem. The DNS code, reported in Lundbladh *et al.*,[24] is used to solve the temporal problem for a parallel Blasius base flow. For a quantitative comparison we analyze the DNS results in terms of an amplitude expansion, so as to isolate the linear, quadratic, and cubic part of the solution, see Henningson *et al.*[25] We in fact run the same case with three different small amplitude disturbances. Different Fourier modes are then extracted and compared with the results obtained using the perturbation model.

We first consider the velocity field at early times, where the problem is governed by Eq. (24) and the initial value problem is solved as a superposition of the discretized eigenmodes. Comparisons of the three velocity component for the Fourier mode $(\alpha,\beta)=(0.2,\ 0.2)$ are shown in Fig. 1 at time $t=100$. The good agreement confirms the validity of the discrete representation of the continuous spectrum. An eigenvalue map for the Orr–Sommerfeld operator, obtained using $N=301$ Chebyshev polynomials, is shown in Fig. 2 together with the exact analytical solution of Eq. (37). The 150 least damped eigenfunctions are taken into account in the expansion presented in Fig. 1. We re-emphasize here that this approximation is able to correctly describe the evolution of disturbances localized in the free stream.

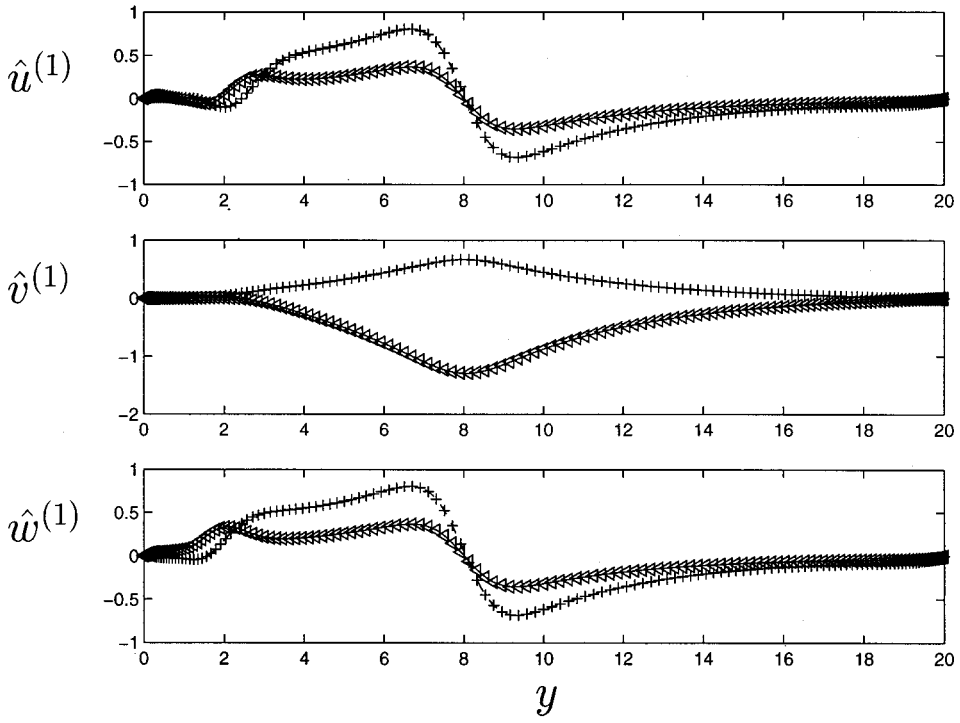


FIG. 1. Velocity components of the linear perturbation velocity for the oblique wave with $(\alpha,\beta)=(0.2,0.2)$. Forced problem for Re=400, $y_\infty=20$, $y_0=8$, $\sigma=0.5$, $\omega=0.2$, and $t=100$. DNS result: +, real part, $\triangleleft$, imaginary part. Perturbation model: - - -, real part; —, imaginary part.

With regards to the asymptotic time behavior, the numerical simulations are run to time $t=50\,000$ and the response is compared with the perturbation results. Figure 3 depicts the velocity components associated to the mode $(\alpha,\beta)=(0.2, 0.2)$. The small differences observed in the figures are probably due to the accumulation of truncation errors in the DNS after such a long time integration. For the same problem, the second order correction with $(0, 2\beta)$ and $\omega=0$ is displayed in Fig. 4. The formation of streamwise streaks in the longitudinal component is clearly seen. A similar result (not reported) is observed in the case of localized forcing inside the boundary layer ($y_0=2.2$, $\sigma=0.4$). However, in the latter case, the streaks exhibit an amplitude smaller than the previous case (about one third).

Let us consider the transient part of the solution. The time evolution of the energy of the response of the forced problems corresponding to two different wave numbers [(0.2, 0.2), (1,1)] and for the same values of $y_0$ and $\sigma$ ($y_0$ ($y_0=8$, $\sigma=0.5$) is shown in Fig. 5. The figure shows that the energy of the high wave number disturbances attains its asymptotic value on a scale that is one order of magnitude less than the one associated to the short wave number (both for the first and the second order corrections).

## IV. ROLE OF CONTINUOUS SPECTRA IN THE RECEPTIVITY MECHANISM

### A. Reynolds number scaling

As shown in Sec. II B, it is possible to prove that the resolvent, which governs the solution to the forced Orr–Sommerfeld, Squire system, is $O(\mathrm{Re}^2)$. For the second problem we address, the forcing is given by nonlinear interactions between continuous spectrum modes, and we analyze the forced solution at different values of the Reynolds number. In Fig. 6 we compare the continuous spectrum modes of the Orr–Sommerfeld operator for $\alpha=1$, $\beta=0.2$ and $\gamma=0.628$ at two different Reynolds numbers (Re=300 and Re=500). We observe that the modes differ only at the edge of the boundary layer and these differences are small. Hence, we assume that the forcing term is Re independent. This assumption is confirmed for large Reynolds number by the findings of Jacobs and Durbin,[23] who have shown that the penetration depth of the modes is proportional to $(\alpha\,\mathrm{Re})^{-0.13}$ which implies that for large values of Re this depth becomes smaller and smaller.

In Fig. 7 we report the plot of the maximum of the streamwise second order velocity (normalized by the first

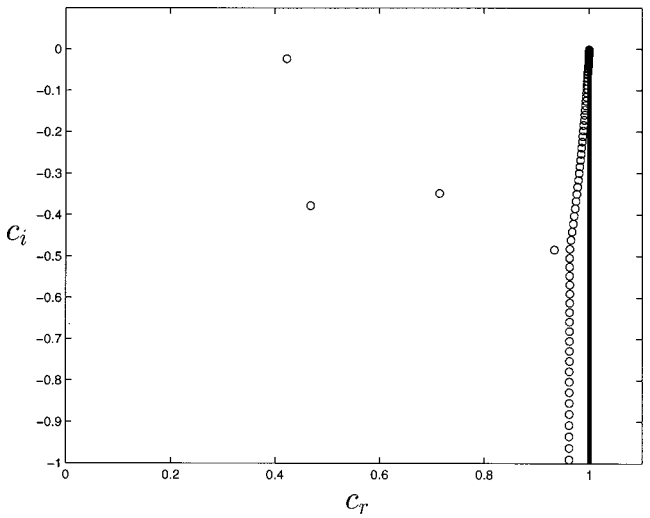


FIG. 2. Numerically obtained Orr–Sommerfeld spectrum: $N=301$ Chebyshev modes, Re=400, $(\alpha,\beta)=(0.2, 0.2)$, and $y_{\max}=20$. The solid line displays the exact continuous spectrum.

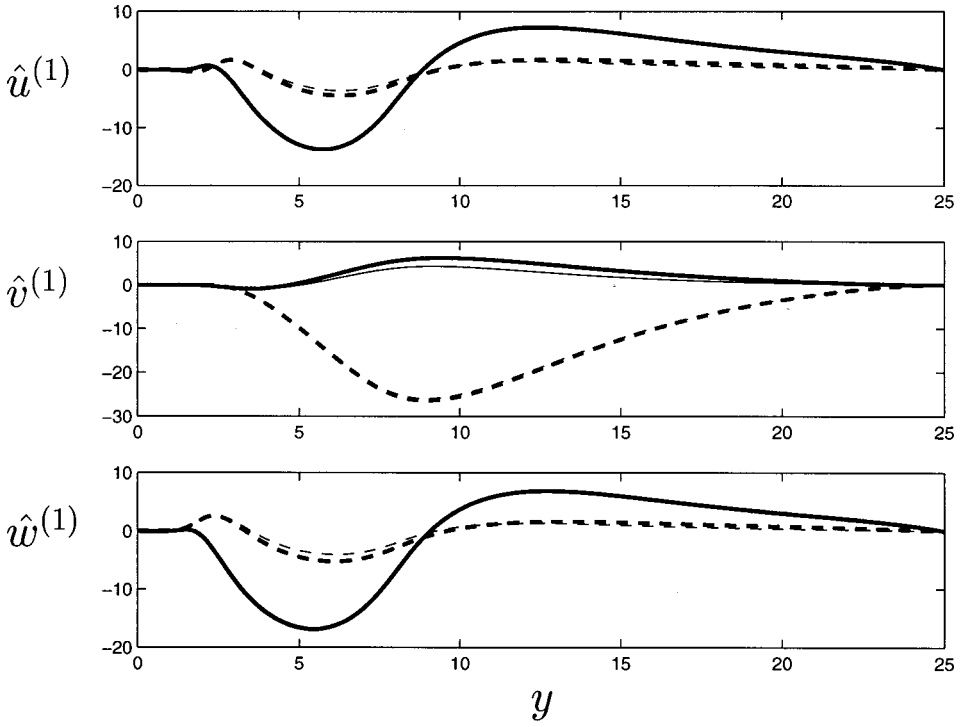


FIG. 3. Velocity components of the linear perturbation velocity for the oblique wave with $(\alpha,\beta)=(0.2, 0.2)$. Forced problem for Re=400, $y_\infty=25$, $y_0=8$, $\sigma=0.5$, $\omega=0.2$, and $t=50\,000$. DNS result: - - -, real part; —, imaginary part (thick lines). Perturbation model: - - -, real part; —, imaginary part (thin lines).

order energy and by the square of Re) as a function of the streamwise and spanwise wave numbers for a given value of $\gamma$, note that the second order distribution is displayed with reference to the $(\alpha,\ \beta)$ values of the corresponding first order terms. The figure clearly confirms the scaling in the energy norm found in Sec. II B. The results show that the maximum amplitude is obtained for $\alpha\approx 2$ and $\beta\approx 0.15$. Further computations (not reported) verify the validity of the scaling down to Re≈100. However, for lower values of the Reynolds number the maximum response is obtained for values of $\beta$ less than the one associated to Re>100. Thus, it suffices to investigate the forced results only at one Reynolds number, since they can be subsequently scaled to arbitrary Re>100.

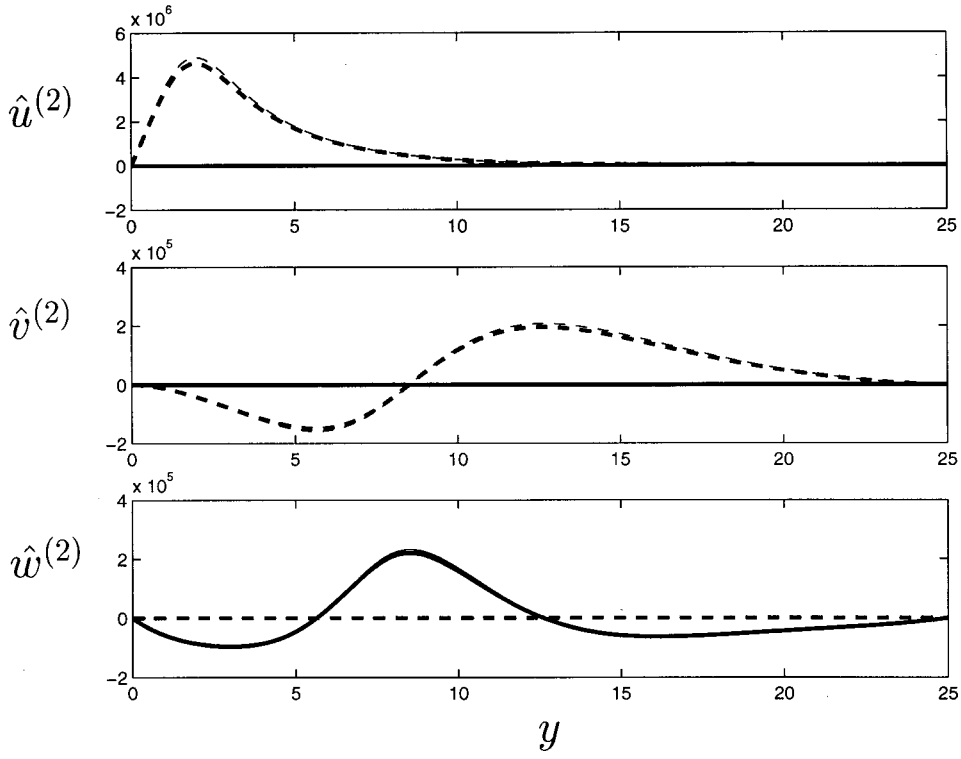


FIG. 4. Velocity components of the second order perturbation velocity for $(\alpha,\beta)=(0, 0.4)$. Forced problem for Re=400, $y_\infty=25$, $y_0=8$, $\sigma=0.5$, and $t=50\,000$. DNS result: - - -, real part; —, imaginary part (thick lines). Perturbation model: - - -, real part; —, imaginary part (thin lines).

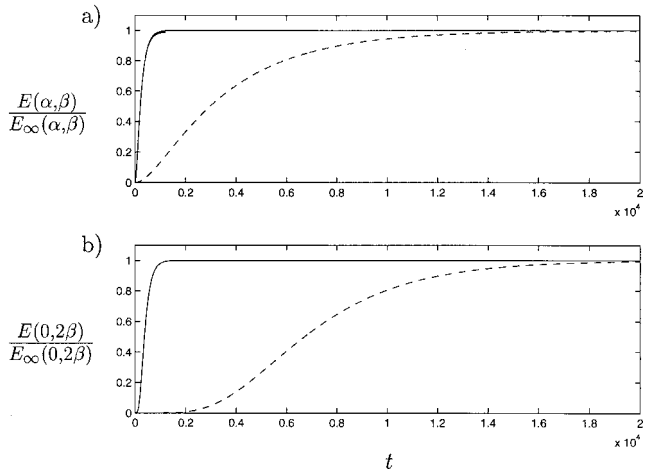


FIG. 5. Time evolution of the energy normalized with respect to its asymptotic value. (a) First order correction; (b), second order correction; —, $(\alpha,\beta)=(1,1)$; - - -, $(\alpha,\beta)=(0.2, 0.2)$.

### B. Nonlinear interaction and linear forcing

In a previous work it has been demonstrated that nonlinearities play a fundamental role in boundary layer receptivity, see Berlin and Henningson.[14] In the present work we use a model based on a perturbation expansion in the amplitude of the disturbance truncated at second order to single out the mechanisms at work during the generation of streamwise streaks in flat plate boundary layers subject to free-stream turbulence.

Since it is possible to rather well represent free-stream turbulence as a superposition of modes associated to the continuous spectrum, see, for example, Jacobs and Durbin,[26] we simplify the problem analyzing the weakly nonlinear response of the system to a single pair of oblique continuous spectrum modes.

First we analyze the problem associated to the Orr–Sommerfeld continuous spectrum modes. The first order solution corresponds to two eigenmodes of the continuous spectrum with wave numbers $(\alpha,\beta,\gamma)$ and $(\alpha,-\beta,\gamma)$ whose damping rate is set to zero. At second order we account for the quadratic interactions between the two continuous spectrum modes and we focus our attention on the $(0, 2\beta)$ contribution. The transient part of the solution is neglected and the asymptotic time response is analyzed. We observe that the second order forcing to the $(0, 2\beta)$ modes induces strong streamwise vorticity, that in turn forces the formation of streaks inside the boundary layer by the linear lift-up mechanism. This two-step process, first the nonlinear generation of streamwise vortices and then the linear forcing of the streamwise streaks, is completely captured by the weakly nonlinear model. Figure 8 shows that the nonlinear forcing of the Orr–Sommerfeld, Squire system [$T_0^L$, shown in Fig. 8(a)] induces second order spanwise and normal to wall velocities [see Fig. 8(b)]. As a consequence, streamwise vorticity is produced which then creates streamwise streaks [see Fig. 8(c)] through the forcing of the Squire equation due to the coupling term [which is approximately 10 times larger than the corresponding second order forcing, compare Figs. 8(a) and 8(d)]. Further, Fig. 8(b) shows that the second order correction in $\hat{v}^{(2)},\hat{w}^{(2)}$ is $O(\mathrm{Re})$ ($|\hat{v}^{(2)}|,|\hat{w}^{(2)}|\approx 600$), while Fig. 8(c) that the streamwise velocity is $O(\mathrm{Re}^2)$ ($|\hat{u}^{(2)}| \approx 17\,000$), confirming the scaling property of the resolvent of the Orr–Sommerfeld and Squire problems discussed at the end of Sec. II B.

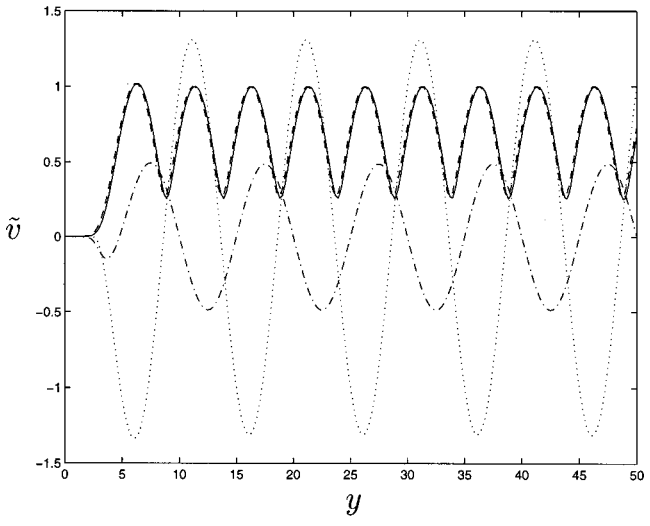


FIG. 6. Distribution of the Orr–Sommerfeld eigenfunction vs $y$ for $\alpha=1$, $\beta=0.2$: —, $\|\tilde{v}\|$ for Re=500; - - -, $\|\tilde{v}\|$ for Re=300; $\cdots$, Re$(\tilde{v})$ for Re =300; $\cdot$ - $\cdot$, Im$(\tilde{v})$ for Re=300.

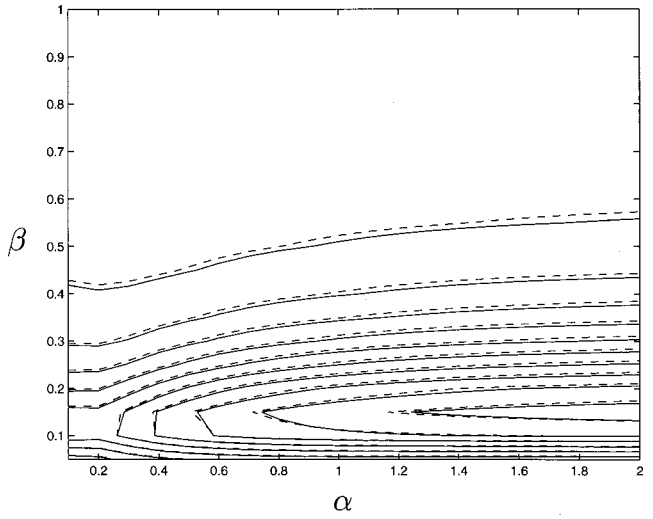


FIG. 7. Forcing induced by Orr–Sommerfeld continuous spectrum modes for $\gamma=0.27$. Contour levels of the maximum of the streamwise second order velocity (normalized by the first order energy and $\mathrm{Re}^2$). Note that the second order distribution is displayed with reference to the $(\alpha,\beta)$ values of the corresponding first order terms. Maximum value 0.1056, contour spacing 0.011.

The same analysis has been carried out also considering the second order forcing induced by Squire continuous spectrum modes. The results show that the same physical mechanism is induced and the amplitude of the generated streaks is comparable for the two different classes of modes.

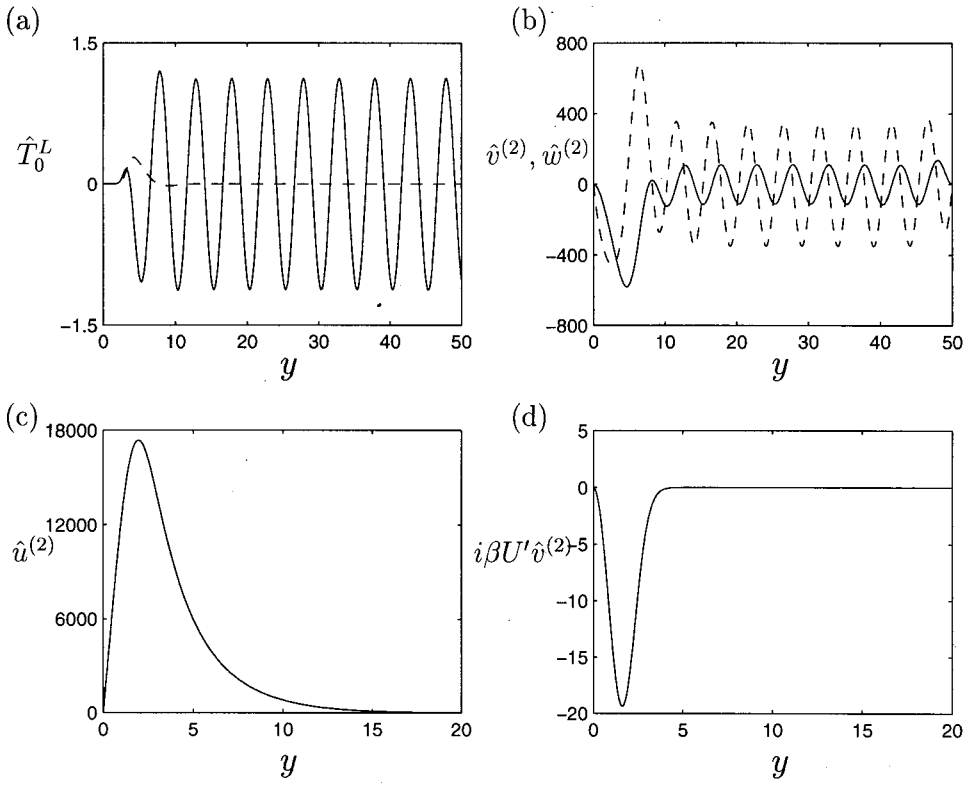


FIG. 8. Second order solution corresponding to the nonlinear interactions of a couple of oblique Orr–Sommerfeld modes associated to the wave numbers (0.5, ±0.2, 0.628), at Re=500: (a) forcing to the Orr–Sommerfeld equation (—) and to the Squire equation (- - -); (b) normal to wall (—) and spanwise component of velocity (- - -); (c) streamwise component of velocity; (d) forcing to the Squire equation associated to the coupling term $-i\beta U' v^{(2)}$.

### C. Parametric study

In order to find the most effective interactions between continuous spectrum modes we carried out a parametric study varying the wave numbers in the range $0.1<\alpha<2$,$0.05<\beta<1$, and $0.25<\gamma<20.9$ at a given Reynolds number. In Figs. 9 and 10 we report, respectively, the results corresponding to forcing induced by Orr–Sommerfeld and Squire continuous spectrum modes. The figures depict the maximum amplifications of the streamwise velocity component normalized with respect to the energy density $E$ of the nonlinearly interacting modes. In particular, we plot

$$A(\alpha,\beta)=\max_\gamma \frac{u^{(2)}(\alpha,\beta,\gamma)}{E},$$

$$B(\alpha,\gamma)=\max_\beta \frac{u^{(2)}(\alpha,\beta,\gamma)}{E},$$

$$C(\beta,\gamma)=\max_\alpha \frac{u^{(2)}(\alpha,\beta,\gamma)}{E}.$$

The results show that the maximum amplification is attained for $\alpha\approx 2$ and $\beta\approx 0.15$ (thus implying that the streaks are associated to spanwise wave number $\beta\approx 0.3$) independently of the type of forcing modes. The results also indicate that the maximum response is associated to low values of $\gamma$ ($\gamma\approx 0.25$), i.e., structures of large wall normal extent. We observe that in the case the forcing is given by the Orr–Sommerfeld modes we find a lower maximum for $\alpha\approx 0.1$, $\beta\approx 0.2$, and $\gamma\approx 1.25$.

One should also note that these figures tend to bias high wave numbers, since they are in practice more damped than low ones. Recall in fact that for simplicity we have put the damping rate of the continuous spectrum modes to zero. This implies, for example, that the increasing amplification for higher values of $\alpha$ in Figs. 9(a), 9(b), 10(a), and 10(b) would be damped for sufficiently high values of the streamwise wave number. However this does not present a problem in applying the results to a real free-stream turbulence case since realistic free-stream turbulence spectra have little energy content in these higher wave numbers. This will be discussed in the next section.

### D. Filtering with turbulent energy spectrum and streak spacing

In the results presented so far we assumed unit energy in each Fourier component of the free-stream disturbance. In order to predict which length scales may be important in a real transition initiated by free-stream turbulence, we associate each mode with a coefficient proportional to the energy spectrum of typical homogeneous and isotropic turbulence. We use here the von Kármán spectrum, which is proportional to $\kappa^4$ for large scales and matches the Kolmogorov-(5/3)-law for small scales. It has the form

$$\tilde{E}^{3D}(\alpha,\beta,\gamma)=\frac{E^{3D}(\kappa_{3D})}{4\pi\kappa_{3D}^2}$$

$$=\frac{2}{3}\frac{1}{4\pi\kappa_{3D}^2}\frac{1.606(\kappa_{3D}L)^4}{(1.35+(\kappa_{3D}L)^2)^{17/6}}Lq, \quad (43)$$

where $\kappa_{3D}=\alpha^2+\beta^2+\gamma^2$, $L$ is an integral length scale and $q$ is the total turbulent kinetic energy, defined as the integral over all $\kappa$'s of the spectrum. It is possible to show that the

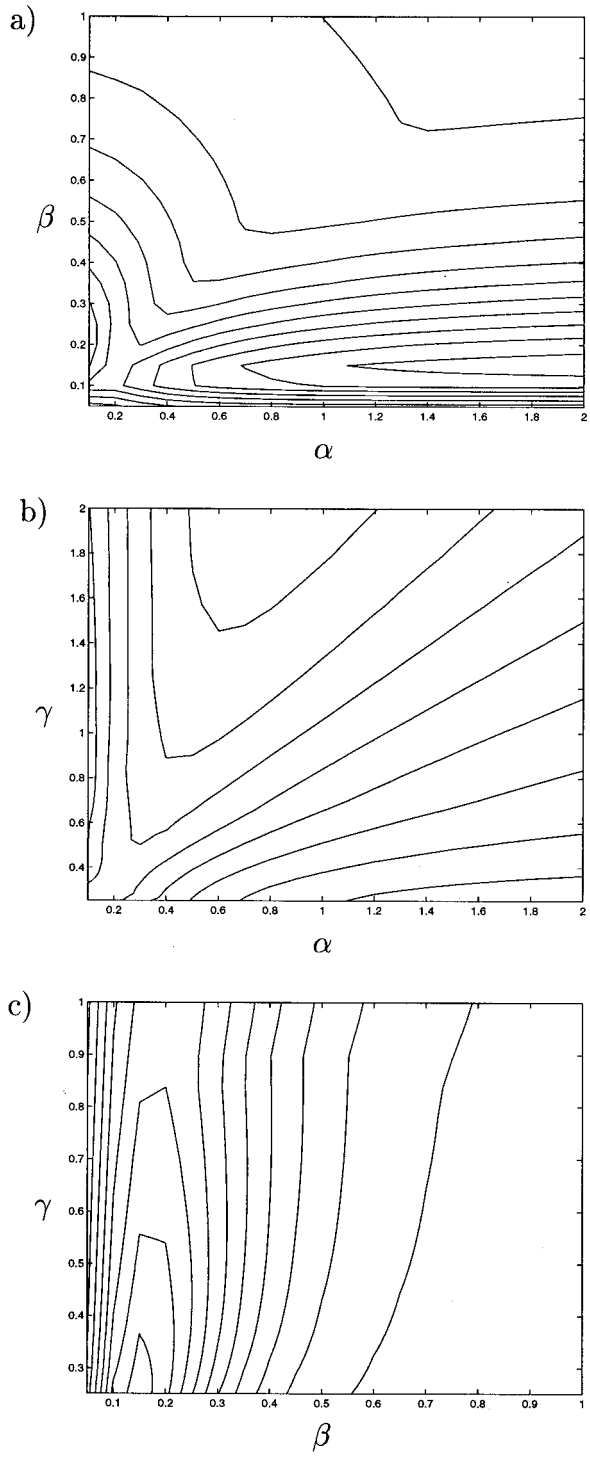


FIG. 9. Boundary layer response to forcing induced by nonlinear interactions of Orr–Sommerfeld modes. Contour levels of the maximum amplification of the streamwise component of velocity at Re=300, $y_\infty=50$: (a) $A(\alpha,\beta)$ for $0.25<\gamma<20.9$; (b) $B(\alpha,\gamma)$ for $0.05<\beta<1$; (c) $C(\beta,\gamma)$ for $0.1<\alpha<2$. The maximum is 10 145 and occurs at $\alpha=2$, $\beta=0.15$, $\gamma=0.25$. Maximum contour level is 9500 and contour spacing 1000.

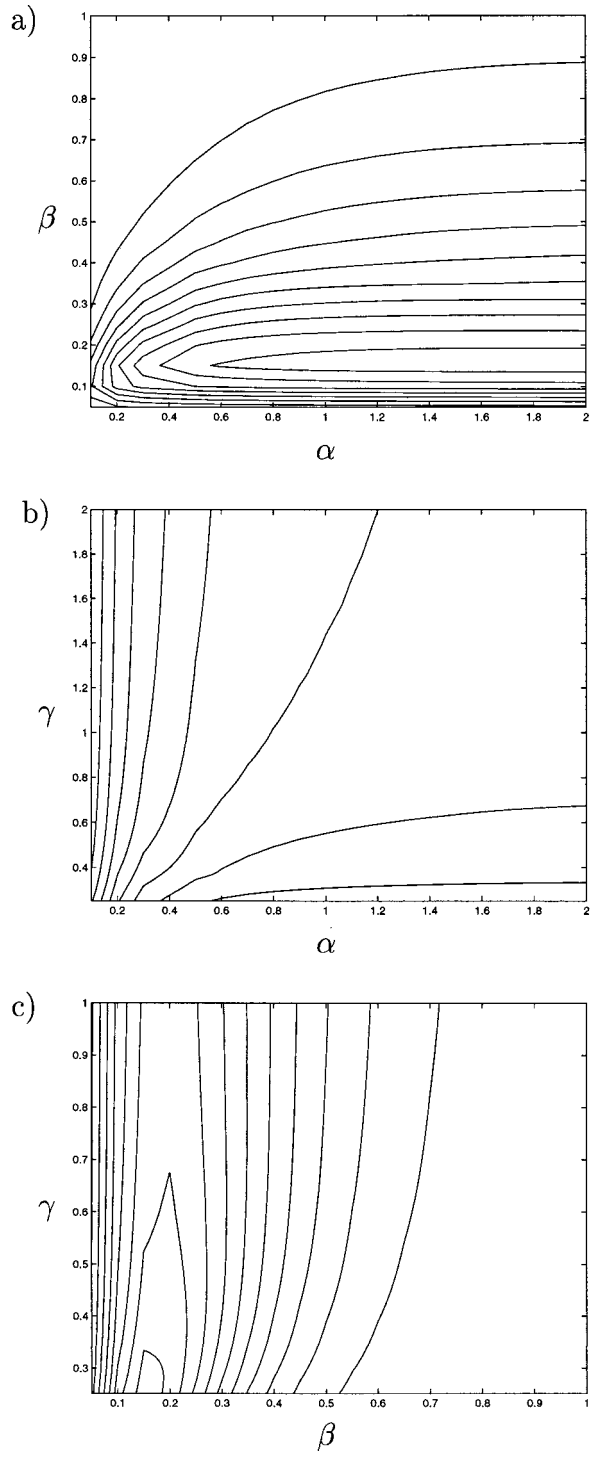


FIG. 10. Boundary layer response to forcing induced by nonlinear interactions of Squire modes. Contour levels of the maximum amplification of the streamwise component of velocity at Re=300, $y_\infty=50$: (a) $A(\alpha,\beta)$ for $0.25<\gamma<20.9$; (b) $B(\alpha,\gamma)$ for $0.05<\beta<1$; (c) $C(\beta,\gamma)$ for $0.1<\alpha<2$. The maximum is 10 586 and occurs at $\alpha=2$, $\beta=0.15$, $\gamma=0.25$. Maximum contour level is 10 000 and contour spacing 1000.

integral length scale $L_{11}\approx 0.65L$ and that the length scale of the eddies with the maximum energy is $L_{\max}\approx 3.5L$. We note that this spectrum, given in Tennekes and Lumley[27] is a good approximation to homogeneous turbulence. The filtered results are reported in Figs. 11 and 12 for $L=3$, $q=1$; the figures show that the filtering moves the more effective $\alpha$'s and $\gamma$'s to smaller values, while the $\beta$'s are less affected. The maximum amplification is attained for $\alpha\approx 0.3$, $\beta\approx 0.1$ for the case the forcing is given by the Orr–Sommerfeld modes and $\alpha\approx 0.3$, $\beta\approx 0.15$ for the Squire case; the corresponding values of $\gamma$ is 0.25 independently of the type of the forcing

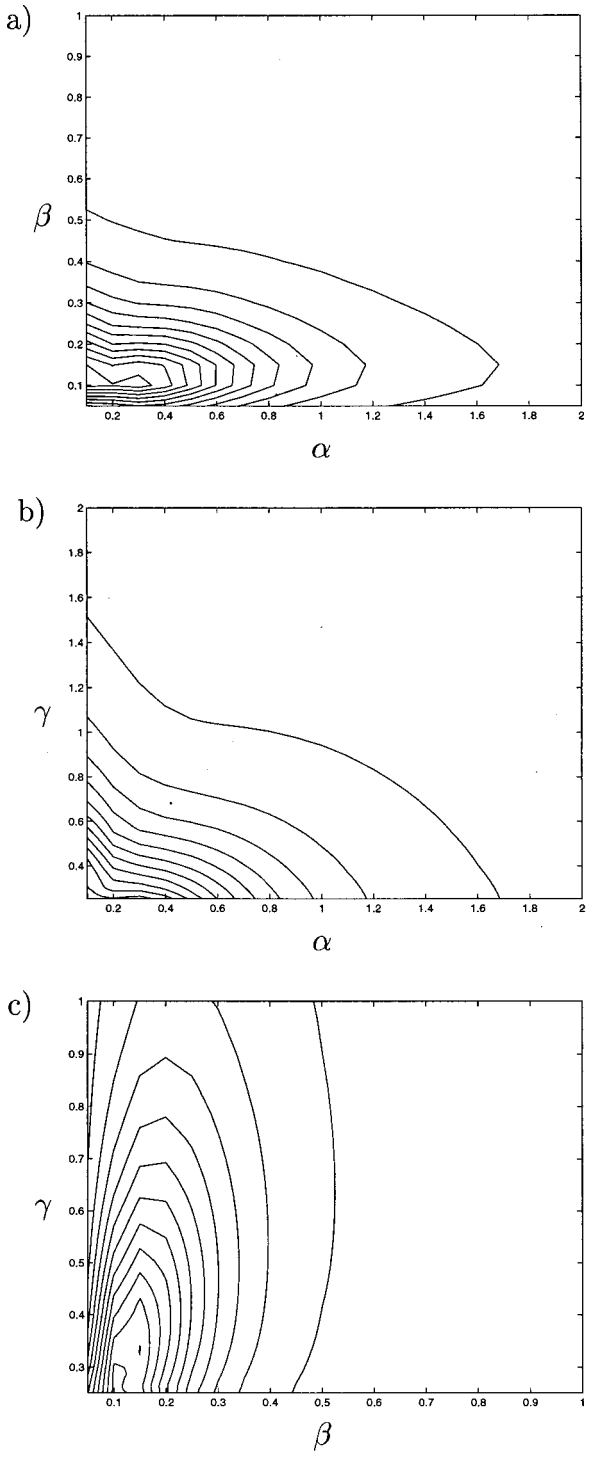


FIG. 11. Boundary layer response to forcing induced by nonlinear interactions of Orr–Sommerfeld modes filtered by turbulent kinetic energy spectrum. Contour levels of the maximum amplification of the streamwise component of velocity at Re=300, $y_\infty=50$: (a) $A(\alpha,\beta)$ for $0.25<\gamma<20.9$; (b) $B(\alpha,\gamma)$ for $0.05<\beta<1$; (c) $C(\beta,\gamma)$ for $0.1<\alpha<2$. The maximum is 1106 and occurs at $\alpha=0.3$, $\beta=0.1$, $\gamma=0.25$. Maximum contour level is 1050 and contour spacing 100.

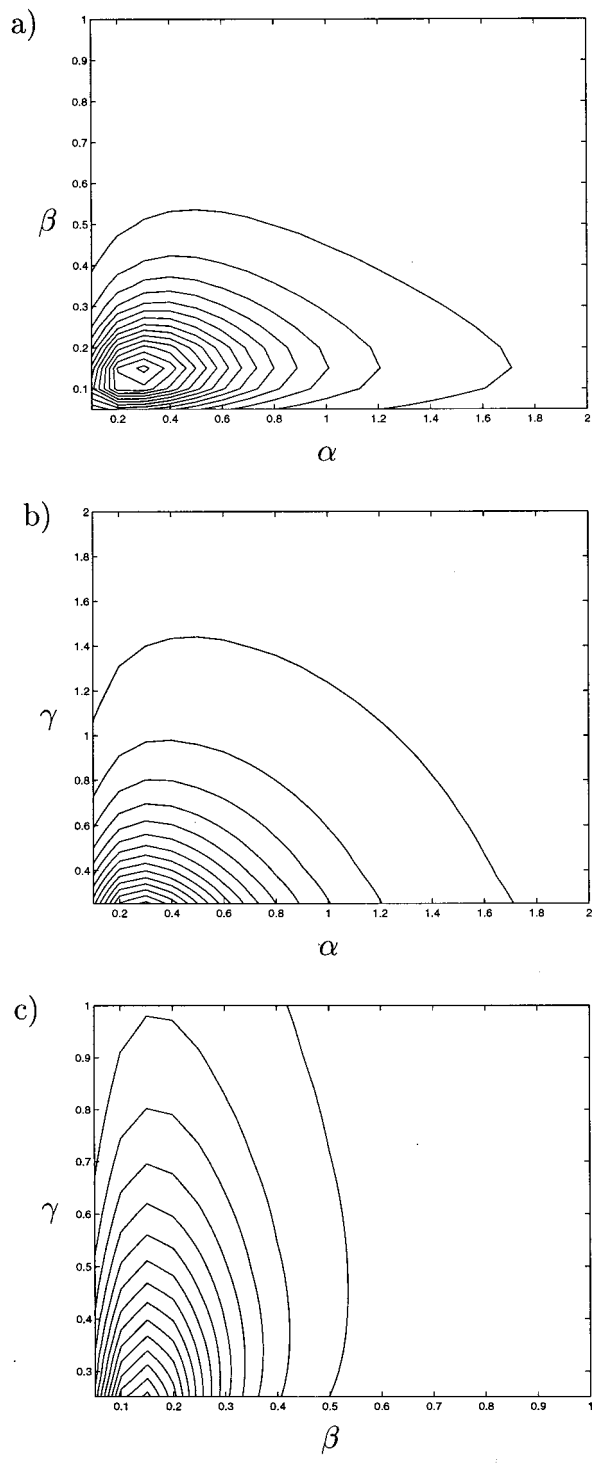


FIG. 12. Boundary layer response to forcing induced by nonlinear interactions of Squire modes filtered by turbulent kinetic energy spectrum. Contour levels of the maximum amplification of the streamwise component of velocity at Re=300, $y_\infty=50$: (a) $A(\alpha,\beta)$ for $0.25<\gamma<20.9$; (b) $B(\alpha,\gamma)$ for $0.05<\beta<1$; (c) $C(\beta,\gamma)$ for $0.1<\alpha<2$. The maximum is 1485 and occurs at $\alpha=0.3$, $\beta=0.15$, $\gamma=0.25$. Maximum contour level is 1450 and contour spacing 100.

modes. We note also that in the case the forcing is given by the Orr–Sommerfeld modes, a lower local maximum is still present at $\alpha\approx0.1$, $\beta\approx0.15$, and $\gamma\approx0.33$. Similar results were obtained for different choices of the integral length scale $L$.

One of the objectives of the present work is to find the wave numbers associated to free-steam disturbances which are most effective in the generations of streamwise vortices. Matsubara and Alfredsson[28] in their experimental work observed that the spanwise distance to the first minimum of two

point velocity correlations, which closely corresponds to half the streak spacing, stays almost constant in the downstream direction. This suggests that the boundary layer growth does not affect the streak development. When scaling these results with the local displacement thickness the characteristic length scale close to the leading edge is approximatively $20\delta^* \pm 10\delta^*$, i.e., centered around a spanwise wave number $\beta \approx 0.3$. This is close to the $\beta$'s for which our simplified temporal model predicts the largest response. In the experiments of Matsubara and Alfredsson[28] the growth of the boundary layer implies a variation of the spanwise scale with the respect to the local displacement thickness. In our model, we do not account for the growth of the boundary layer, but we are still able to predict the first step of the receptivity process, i.e., the formation of streamwise vortices.

### E. Linear vs nonlinear receptivity

A linear mechanism for streak generation caused by the diffusion of a free-stream streamwise vortex into the boundary layer has been studied by Andersson *et al.*[11] and Luchini,[12] using the boundary layer equations and by Wundrdow and Goldstein[13] by means of asymptotic expansions. These studies assume the presence of the vortex at the leading edge. Bertolotti[10] used a different method to calculate the initial streamwise vortices, but still studied a linear mechanism. Here we propose a nonlinear model for receptivity, originating from oblique modes in the free stream, with forcing at order $\epsilon^2$, and in this section we want to discuss the relevance of the proposed mechanism in comparison with the stronger direct forcing at order $\epsilon$ presented in the works cited above.[10–13]

Our results show that modes in a wide range of wave numbers $\alpha$, $\beta$, $\gamma$ are almost equally effective in inducing streamwise streaks (see Figs. 9 and 10). On the other hand, for the linear mechanism to work, only streamwise or almost independent modes, with a definite spanwise modulation, can be considered. Therefore in a real case of free-stream turbulence, it is plausible to assume that larger total forcing is involved in the nonlinear process than in the linear one. To quantify, we consider the turbulent kinetic energy spectrum for homogeneous and isotropic turbulence defined by Eq. (43). Frequency spectra of the free-stream turbulence are usually reported from laboratory measurements. By Taylor hypothesis they can be related to one-dimensional spectra for the streamwise wave number $\alpha$. Formally the one-dimensional spectrum $E^{1D}$ is obtained from $E^{3D}$ by

$$E^{1D}(\kappa_{1D}) = \int_{\kappa_{1D}}^{\infty} \frac{E^{3D}}{\kappa_{3D}} \left(1 - \frac{\kappa_{1D}^2}{\kappa_{3D}^2}\right) d\kappa_{3D},$$

see Hinze;[29] it represents the energy in all the Fourier components with wave number $\kappa_{1D}$, corresponding to $\alpha$, $\beta$ or $\gamma$ (since the turbulence is assumed to be isotropic). The one-dimensional spectrum derived from the expression in Eq. (43) can be written as

$$E^{1D}(\kappa_{1D}) = \frac{18}{55} \frac{1.606}{(1.35 + (\kappa_{1D}L)^2)^{5/6}} Lq.$$

Here instead, we want to look at the energy in each plane wave characterized by wave number $(\alpha, \beta)$. A two-dimensional energy spectrum can be defined according to

$$\tilde{E}^{2D}(\alpha,\beta) = \int_{-\infty}^{\infty} \tilde{E}^{3D} d\gamma = \frac{E^{2D}(\kappa_{2D})}{2\pi\kappa_{2D}},$$

with $\kappa_{2D}^2 = \alpha^2 + \beta^2$, which yields in our case

$$E^{2D}(\kappa_{2D}) = 2\pi\kappa_{2D} \times \frac{1.606 L^{1/3} \left(\frac{L^2}{1.35 + L^2\kappa_{2D}^2}\right)^{1/3} (4.05 + 11L^2\kappa_{2D}^2)\Gamma(1/3)}{165\sqrt{\pi}(1.35 + L^2\kappa_{2D}^2)^2\Gamma(5/6)} Lq,$$

where $\Gamma$ represents the gamma function. The three energy spectra versus the respective wave vector are displayed in Fig. 13 for $L=3$ and the total energy $q=1$. We can now estimate the amount of energy involved in the linear, $\tilde{E}_L$, and in the nonlinear mechanism, $\tilde{E}_{NL}$. Values of the spanwise wave number $\beta$ of the generated streaks are assumed to be in the range $\beta \in [\beta_0, \beta_1]$. In the linear scenario, only the contribution from waves with low values of $\alpha$ is considered, such that

$$\tilde{E}_L = 4 \int_0^{\alpha_0} d\alpha \int_{\beta_0}^{\beta_1} \tilde{E}^{2D} d\beta,$$

where $\alpha$ and $\beta$ assume only positive values and the factor 4 in front of the integral is justified by the symmetry of the function $\tilde{E}^{2D}$. In the nonlinear case oblique waves are considered: the integral is now evaluated for larger values of $\alpha$ and the corresponding range of $\beta$,

$$\tilde{E}_{NL} = 4 \int_{\alpha_0}^{\alpha_1} d\alpha \int_{\beta_0/2}^{\beta_1} \tilde{E}^{2D} d\beta.$$

The ratio between the two energies is then a function of the integral length scale $L$ and of the integration limits, $\tilde{E}_{NL}/\tilde{E}_L = (\tilde{E}_{NL}/\tilde{E}_L)(\alpha_0, \alpha_1, \beta_0, \beta_1, L)$. We can let $\beta_1, \alpha_1 \to \infty$, since the energy spectrum is decaying for large wave numbers. We also assume for simplicity $\alpha_0 = \beta_0$, such that $\tilde{E}_{NL}/\tilde{E}_L = (\tilde{E}_{NL}/\tilde{E}_L)(\alpha_0, L)$. Contour levels of $\log_{10}(\tilde{E}_{NL}/\tilde{E}_L)$ are displayed in Fig. 14. One can note that the largest value $(\tilde{E}_{NL}/\tilde{E}_L = 7331)$ is attained for the lowest

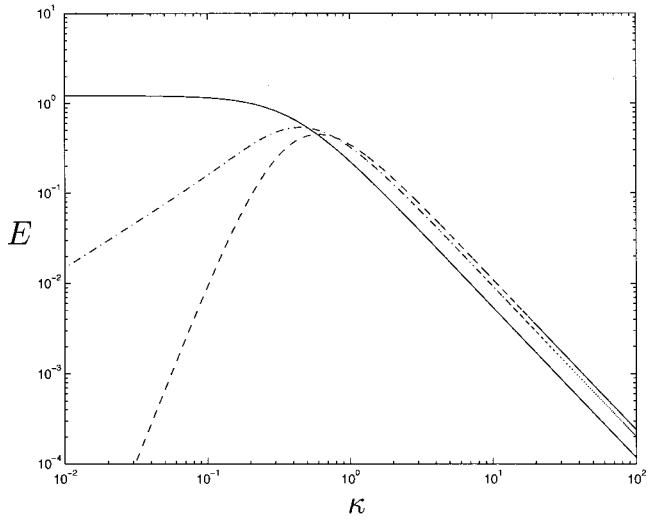


FIG. 13. Turbulent kinetic energy spectra in homogeneous isotropic turbulence. —, $E^{1D}(\kappa_{1D})$; -·-·-, $E^{2D}(\kappa_{2D})$; - - -, $E^{3D}(\kappa_{3D})$.

values of $L$ and $\alpha_0$ considered (1 and 0.0005, respectively) and the ratio decreases for increasing values of the parameters. In Kendall's experiments,[30] with a free-stream velocity $U_\infty = 11$ m/s, the $u_{\rm rms}$, representing the streak's profile, was obtained by filtering at values of 4 and 6 Hz. Using Taylor hypothesis, these values can be transformed to nondimensional values of $\alpha_0 \approx 0.001, 0.0015$ for $\mathrm{Re}_{\delta^*} = 300$. In this range, the energy in modes responsible for the linear receptivity process is about 500 times lower than the energy involved in the nonlinear process.

We have shown that the nonlinear receptivity mechanism can be seen as a two-step process: first the generation of streamwise vortices and then the formation of streaks via lift-up effect. As seen in Fig. 8(b), a strong, $O(\mathrm{Re})$, amplification is associated to the generation of streamwise vortices from nonlinear interaction of oblique modes. The successive formation of streaks is a linear process, present in both the linear and the nonlinear scenario, induced by streamwise vortices of order $\epsilon$ and $\epsilon^2$, respectively. We can then assume that the strong amplification of streamwise vortices can partially compensate the order $\epsilon$ difference between the two, yielding streaks of similar amplitudes. Evidence for this can be found considering the results of the direct numerical simulations presented in Berlin and Henningson,[14] where streaks of the same order of magnitude are generated by the linear and the nonlinear mechanism for an initial energy corresponding to a $v_{\rm rms}$ of about 1%.

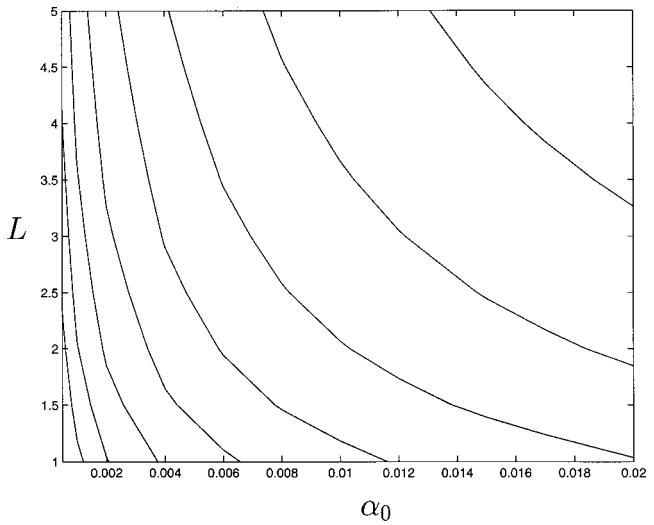


FIG. 14. Isocontours of $\log_{10}(\tilde{E}_{NL}/\tilde{E}_L)$ as function of $L$ and $\alpha_0$. Maximum contour level is 3.5 and contour spacing 0.25. The maximum of $\tilde{E}_{NL}/\tilde{E}_L$ is 7331.21 and occurs at $L=1$, $\alpha_0 = 0.0005$ (lower left-hand corner).

Numerical evidence of the proposed nonlinear receptivity can be found in the simulations of bypass transition in a boundary layer subject to free-stream turbulence performed by Jacobs and Durbin.[26] They used modes of the continuous spectrum to represent homogeneous isotropic turbulence at the inflow of the computational domain ($\mathrm{Re}_{\delta^*} = 274$). The free-stream turbulent intensity was chosen to correspond with the experiment by Roach and Brierly[31] and ensemble-averaged numerical data are in good agreement with laboratory measurements. Jacobs and Durbin have also shown that the lowest frequency in the synthesized inlet spectrum is far higher than the dominant ones in the region of laminar streaks, i.e., zero energy initially in the zero or almost frequency modes, so that a linear receptivity mechanism can be excluded. Frequencies below those introduced at the inlet can only be generated by nonlinear interactions; hence the nonlinear receptivity mechanism is clearly capable of inducing strong streaks. On the other hand, we have to consider also the work of Bertolotti and Kendall[30] which represents the opposite extreme, i.e., when only low frequency streamwise vortices are introduced in the free stream. In this case, experiments under controlled conditions provided a validation of the linear model presented in Bertolotti.[10] In actual free-stream turbulence induced transition, both types of disturbances are present and it would depend on the amount of energy in low frequency disturbances whether the linear or the nonlinear mechanism dominates. The two mechanisms could interact and cooperate, with the linear one maybe dominating at the leading edge and the nonlinear forcing more active further downstream. This is still an open question and the object of future investigations.

## V. DISCUSSION AND CONCLUSION

In the present work we have investigated how free-stream disturbances affect a laminar boundary layer. In particular, we have analyzed the receptivity to oblique waves in the free stream and to continuous spectrum modes. In both cases, we observe that the formation of streaks is the dominant feature. The underlying mechanism can be reduced to a two-step process, first the generation of streamwise vorticity and then the formation of streaks.

Previous investigators[10–13] have considered the influence of streamwise vortices present in the free stream and have shown that the subsequent formation of streaks in the boundary layer can be explained in terms of linear theory by the lift-up mechanism. The most important feature of the process we have investigated is that the same streamwise vortices undergoing algebraic growth, are nonlinearly generated start-

ing from wave-like disturbances in the free stream. As discussed in Sec. IV E, linear and nonlinear receptivity mechanisms are both capable of generation of streaks. In the first case, streamwise independent vortices of small amplitude $\epsilon$, already present in the free-stream disturbance, are able to penetrate the boundary layer, mainly close to the leading edge. In the second, the streamwise vorticity is induced at order $\epsilon^2$ by nonlinear interactions of free-stream disturbances also downstream of the leading edge. Which of the two is dominating in a real case, will depend on the energy content in low frequency modes of the free-stream turbulence.

The nonlinear mechanism has already been observed in the numerical experiments of Berlin and Henningson.[14] They isolated the different order interactions to show that the streamwise independent modes are the most excited. Here, we have used a perturbation expansion which has been shown to provide an efficient theoretical tool to isolate the two-step process, see also Ponziani *et al.*[16] Formally the present model is valid for small amplitudes $\epsilon$ of the perturbation. As in all asymptotic expansions, the actual value of the small parameter $\epsilon$ that can be used, can only be determined empirically. In this case, considering the works of Berlin and Henningson[14] and Jacobs and Durbin,[26] it seems that a turbulence level of 3% is small enough for the model to apply. Further, in Ponziani *et al.*,[16] good agreement between DNS and the nonlinear model is obtained for plane Poiseuille flow for a value of $\epsilon=0.05$. For larger values of free-stream turbulence we expect the nonlinear scenario to become even more important, but it cannot be correctly captured by an amplitude expansion like the one we considered.

The model has been validated by comparisons with DNS data for the case the forcing is given by a couple of oblique waves. In order to apply the model to study the boundary layer receptivity to free-stream turbulence, we have exploited the fact that continuous spectrum modes can be used to represent the free-stream turbulence spectrum.[26] This assumption has allowed us to further simplify the study accounting only for the response of the boundary layer to couples of continuous spectrum modes. An extensive parametric study has been carried out to isolate the most effective modes by varying the wave numbers $(\alpha,\beta,\gamma)$.

We have concluded that the formation of streaks is due to the second order correction induced by the coupling term in the Orr–Sommerfeld, Squire system and the receptivity is independent of the type of forcing modes. This indicates that disturbances containing normal velocity in the free-stream, are not more likely to force streamwise vorticity in the boundary layer, compared to disturbances not containing $v$. On the other hand, Berlin and Henningson[14] draw the conclusion that the normal velocity in the free stream is more effective than other components. However, their conclusion was based on a type of disturbance which grew in size in the normal direction as the normal velocity increased. Thus their results are also consistent with the present ones which show that this increase in amplification is rather a result of increase in normal scale (or decrease in $\gamma$).

The large eddy simulations of Yang and Voke[32] also indicated the key influence of the wall normal component of the free-stream turbulence intensity in provoking transition. Their results show in fact that the transition process begins with the production of the Reynolds stresses due to the overlapping of regions of nonzero fluctuating velocity $v$ and mean shear $\partial U/\partial y$. From our analysis we find that the components with streamwise wave number approximately zero are the ones crucial in generating disturbances inside the boundary layer, and that can be induced from nonlinear interactions of either Orr–Sommerfeld or Squire modes. The capability of modes with frequency and streamwise wave number approximately zero to penetrate the shear layer has been demonstrated by different authors,[3,23,28,33] and we may thus conclude that $v$ components active in generating Reynolds stresses are the ones associated with nearly zero frequency and that they are the ones associated with the second order solution in our model.

The results also show that the second order forcing does not depend on the Reynolds number, thus recovering the $O(\mathrm{Re}^2)$ scaling of the forced response described by streamwise independent disturbances governed by the Orr–Sommerfeld, Squire system. We may speculate on the implication of this scaling on the Reynolds number dependence of the forced response in the spatial problem. In a number of experiments it has been seen that the growth of the streak amplitude in boundary layers subjected to free-stream turbulence is proportional to Re, or equivalently that the energy growth is proportional to $\mathrm{Re}_x \approx \mathrm{Re}^2$ or downstream distance. If we assume that the Reynolds number dependence in the spatial case would be the same as in the temporal case investigated here, downstream growth of the streak amplitude predicted would be proportional to $\mathrm{Re}^2$, i.e., over predicted by a factor of Re. However, the result found here assumes a continuous deterministic forcing. Real turbulence would better be described by a stochastic forcing in a number of wave numbers. Bamieh and Dahleh[34] have shown that a stochastic forcing reduces the scaling of the maximum response of the temporal problem from $\mathrm{Re}^2$ to $\mathrm{Re}^{3/2}$. This is still a factor $\mathrm{Re}^{1/2}$ too large. However, the growth in a realistic free-stream turbulence case would probably further be reduced by the fact that free-stream turbulence decays with downstream distance. In our model this would correspond to a forcing which decreases with Re, thus further reducing the growth of the streak amplitude.

## ACKNOWLEDGMENTS

This research was supported by the Göran Gustavsson Foundation, TFR (Teknikvetenskapliga forskningsrådet), the C. M. Lerici Foundation and the research funding obtained by Professor R. Piva, University of Rome ''La Sapienza.''

[1] P. S. Klebanoff, ''Effect of free-stream turbulence on the laminar boundary layer,'' Bull. Am. Phys. Soc. **10**, 1323 (1971).
[2] J. M. Kendall, ''Experimental study of disturbances produced in a pretransitional laminar boundary layer by weak free-stream turbulence,'' AIAA Pap. 85–1695 (1985).
[3] K. J. A. Westin, A. V. Boiko, B. G. B. Klingmann, V. V. Kozlov, and P. H. Alfredsson, ''Experiments in a boundary layer subject to free-stream turbulence. Part I: Boundary layer structure and receptivity,'' J. Fluid Mech. **281**, 193 (1994).

[4]L. H. Gustavsson, ''Energy growth of three-dimensional disturbances in plane Poiseuille flow,'' J. Fluid Mech. **224**, 241 (1991).
[5]K. M. Butler and B. F. Farrell, ''Three-dimensional optimal perturbations in viscous shear flow,'' Phys. Fluids A **4**, 1637 (1992).
[6]S. C. Reddy and D. S. Henningson, ''Energy growth in viscous channel flows,'' J. Fluid Mech. **252**, 209 (1993).
[7]L. N. Trefethen, A. E. Trefethen, S. C. Reddy, and T. A. Driscoll, ''Hydrodynamic stability without eigenvalues,'' Science **261**, 578 (1993).
[8]M. E. Goldstein and L. S. Hultgren, ''Boundary-layer receptivity to long-wave free-stream disturbances,'' Annu. Rev. Fluid Mech. **21**, 137 (1989).
[9]E. J. Kerschen, ''Boundary layer receptivity theory,'' Appl. Mech. Rev. **43**, S152 (1990).
[10]F. P. Bertolotti, ''Response of the Blasius boundary layer to free-stream vorticity,'' Phys. Fluids **9**, 2286 (1997).
[11]P. Andersson, M. Berggren, and D. Henningson, ''Optimal disturbances and bypass transition in boundary layers,'' Phys. Fluids **11**, 134 (1999).
[12]P. Luchini, ''Reynolds number independent instability of the boundary layer over a flat surface: optimal perturbations,'' J. Fluid Mech. **404**, 289 (2000).
[13]D. W. Wundrow and M. E. Goldstein, ''Effect on a laminar boundary layer of small-amplitude streamwise vorticity in the upstream flow,'' J. Fluid Mech. **426**, 229 (2001).
[14]S. Berlin and D. S. Henningson, ''A nonlinear mechanism for receptivity of free-stream disturbances,'' Phys. Fluids **11**, 3749 (1999).
[15]D. Ponziani, Ph.D. thesis, University of Rome, La Sapienza, 2000.
[16]D. Ponziani, C. M. Casciola, F. Zirilli, and R. Piva, ''Weakly nonlinear analysis of a localized disturbance in Poiseuille flow,'' Stud. Appl. Math. **105**, 121 (2000).
[17]A. Tumin and E. Reshokto, ''Spatial theory of optimal disturbances in boundary layers,'' Phys. Fluids **13**, 2097 (2001).
[18]G. Kreiss, A. Lundbladh, and D. S. Henningson, ''Bounds for threshold amplitudes in subcritical shear flows,'' J. Fluid Mech. **270**, 175 (1994).
[19]R. C. DiPrima and G. J. Habetler, ''A completeness theorem for non-selfadjoint eigenvalue problems in hydrodynamic stability,'' Arch. Ration. Mech. Anal. **32**, 218 (1969).
[20]H. Salwen and C. E. Grosch, ''The continuous spectrum of the Orr–Sommerfeld equation. Part 2. Eigenfunction expansions,'' J. Fluid Mech. **104**, 445 (1981).
[21]C. E. Grosch and H. Salwen, ''The continuous spectrum of the Orr–Sommerfeld equation. Part 1. The spectrum and the eigenfunctions,'' J. Fluid Mech. **87**, 33 (1978).
[22]P. J. Schmid and D. S. Henningson, *Stability and Transition in Shear Flows* (Springer, New York, 2001).
[23]R. G. Jacobs and P. A. Durbin, ''Shear sheltering and continuous spectrum of the Orr–Sommerfeld equation,'' Phys. Fluids **10**, 2006 (1998).
[24]A. Lundbladh, S. Berlin, M. Skote, C. Hildings, J. Choi, J. Kim, and D. S. Henningson, ''An efficient spectral method for simulation of incompressible flow over a flat plate TRITA-MEK,'' Technical Report 1999.11, Royal Institute of Technology, Stockholm, 1999.
[25]D. S. Henningson, A. Lundbladh, and A. V. Johansson, ''A mechanism for bypass transition from localized disturbances in wall-bounded shear flows,'' J. Fluid Mech. **250**, 169 (1993).
[26]R. G. Jacobs and P. A. Durbin, ''Simulations of bypass transition,'' J. Fluid Mech. **428**, 185 (2001).
[27]H. Tennekes and J. L. Lumley, *A First Course in Turbulence* (MIT Press, Cambridge, MA, 2000).
[28]M. Matsubara and P. H. Alfredsson, ''Disturbance growth in boundary layers subjected to free stream turbulence,'' J. Fluid Mech. **430**, 149 (2001).
[29]J. O. Hinze, *Turbulence* (McGraw-Hill, New York, 1959).
[30]F. P. Bertolotti and J. M. Kendall, ''Response of the Blasius boundary layer to controlled free-stream vortices of axial form,'' AIAA Pap. 97-2018 (1997).
[31]P. E. Roach and D. H. Brierly, ''The influence of a turbulent freestream on zero pressure gradient transitional boundary layer development, Part I: test cases T3A and T3B,'' *ERCOFTAC Workshop: Numerical Simulations of Unsteady Flows and Transition to Turbulence, Lausanne, Switzerland* (Cambridge University Press, Cambridge, MA, 1990), pp. 319–347.
[32]Z. Y. Yang and P. R. Voke, ''Large eddy simulation of transition under turbulence,'' Technical Report ME-FD/93.12, University of Surrey, Department of Mechanical Engineering, 1993.
[33]L. S. Hultgren and L. H. Gustavsson, ''Algebraic growth of disturbances in a laminar boundary layer,'' Phys. Fluids **24**, 1000 (1981).
[34]B. Bamieh and M. Dahleh, ''Disturbance energy amplification in three-dimensional channel flows,'' *Proceedings of the 1999 American Control Conference* (IEEE, Piscataway, NJ, 1999), pp. 4532–4537.